2017년 2월

석사학위 논문

G9a inhibition by BIX01294 ameliorates neuronal differentiation and degeneration

조선대학교 대학원

생명과학과

김 호 태

G9a inhibition by BIX01294 ameliorates neuronal differentiation and degeneration

BIX01294 (G9a inhibitor)를 이용한 신경분화 및 퇴화 제어

2016년 2월 24일

조선대학교 대학원

생명과학과

김 호 태

G9a inhibition by BIX01294 ameliorates neuronal differentiation and degeneration

지도교수 조 광 원

이 논문을 이학석사학위 신청 논문으로 제출함

2016년 10월

조선대학교 대학원

생명과학과

김 호 태

김호태의 석사학위논문을 인준함

위원장 조선대학교 교수 전택중 (인)

위 원 조선대학교 교수 이준식 (인)

위 원 조선대학교 교수 조광원 (인)

2016년 11월

조선대학교 대학원

CONTENTS

LIST OF FIGURES ····· i
LIST OF TABLE ····· ii
ABBREVIATIONS ····· iii
ABSTRACT ····· 1
국문초록 ····· 3

Part 1
I Introduction ····· 4
II. Materials and Methods ····· 6
II-1. Characteristics of primary human BM-MSCs and cell culture ····· 6
II-2. Quantitative PCR (real-time PCR) ····· 6
II-3. MTT assay ····· 9
II-4. Immunoblotting ····· 9
II-5. Chromatin immunoprecipitation ····· 9
II-6. Neuronal differentiation ····· 11
II-7. Immunocytochemical stanining ····· 11
II-8. Statistical analysis ····· 12
III. Results ····· 13
III-1. Neuroprogenitor genes are induced by BIX01294 in human BM-MSCs ····· 13
III-2. G9a inhibition stimulates the expression of neuronal

specific genes containing RE-1 sequences in BM-MSCs 15
III-3. BIX01294-pretreated BM-MSCs have a neuronal appearance in neuronal induction medium 18
III-4. Significantly increased expression of diverse neuronal markers in neuronal differentiated BIX-MSCs 22
IV. Discussion 24

Part II

I Introduction 26
II. Materials and Methods 27
II-1. Cell culture 27
II-2. MTT assay 27
II-3. Quantitative PCR (real-time PCR) 28
II-4. Immunoblotting 30
II-5. Chromatin immunoprecipitation 30
II-6. Neuronal differentiation 31
II-7. Statistical analysis 31
III. Results 32
III-1. BIX01294 has the protective effects on apoptosis by oxidative stress in neural cells 32
III-2. Downregulation of RE-1 containing neuronal genes by oxidative stress was caused by the activation of G9a 35

lll-3. G9a inhibition was prevented the neuronal cell dysfunction by H_2O_2 ····· 38
lV. Discussion ····· 40
CONCLUSION ····· 42
REFERENCES ····· 43
감사의 글 ····· 48

LIST OF FIGURES

Part I

Figure 1. The expression of neuroprogenitor genes was induced in BIX01294-treated BM-MSCs·····14
Figure 2. The RE-1 containing neuronal specific genes are increase expressed in BIX-MSCs·····16
Figure 3. Neuron-like morphological changes in BIX-MSCs followed by neuronal induction·····18
Figure 4. Increased expression of diverse neuronal markers in differentiated BIX-MSCs·····23

Part II

Figure 1. Protective effects of BIX01294 in oxidative damaged neuronal cell·····34
Figure 2. G9a inhibition was against H_2O_2 - induced decrease of neuronal specific genes·····37
Figure 3. Decline of neuronal differentiation in H_2O_2 treated SH-SY5Y cells and recovery by G9a inhibition·····39

LIST OF TABLE

Part I

Table 1. Oligonucleotides used for real-time PCR·····8
Table 2. Genes containing the consensus sequences of repressor element-1. Chr indicates chromosome·····17
Table 3. The neuronal-like cells were counted to estimate the neuronal differentiation·····20
Table 4. The number of neurites from each differentiated cells were counted and neurite lengths were measured·····21

Part II

Table 1. Oligonucleotides used for real-time PCR·····29

ABBREVIATIONS

BDNF	brain-derived neurotrophic factor
BHA	butylated hydroxyanisole
BIX-MSCs	BIX01294-treated MSCs
BM-MSCs	bone marrow mesenchymal stem cells
ChIP	Chromatin immunoprecipitation
Ctrl-MSCs	control MSCs
dMSCs	differentiated MSCs
dSH-SY5Y	differentiated SH-SY5Y cells
DMSO	dimethyl sulfoxide
FBS	fetal bovine serum
H3K9	lysine 9 on histone 3
MSCs	mesenchymal stem cells
MTT	3(4,5-Dimethylthiazol-2-yl-) 2,5-diphenyltetrazolium bromide
PBS	phosphate buffered saline
PCR	polymerase chain reaction
qPCR	quantitative PCR (or real-time PCR)
RA	Retinoic acids
RE-1	repressor element-1
REST	RE-1 silencing transcription factor
RT	room temperature
SAM	S-adenosyl-L-methionine
SD	standard deviation

ABSTRACT

G9a inhibition by BIX01294 ameliorates neuronal differentiation and degeneration

Ho-Tae Kim
Advisor : Associate Prof. Goang-Won Cho, Ph.D.
Departmant of life science,
Graduate School of Chosun University

Recent studies have shown that epigenomic modifications are significantly associated with neuronal differentiation. Many neuronal specific genes contain the repressor element-1 (RE-1), which recruits epigenetic modulators such as the histone methyltransferase G9a and interrupts the expression of neuronal genes in non-neuronal cells. This study investigated the functional role of G9a during neuronal differentiation of human bone marrow mesenchymal stem cells (BM-MSCs). Human BM-MSCs treated with BIX01294 as G9a inhibitor showed an increased expression of various neuronal-lineage genes. Using genomic sequence analysis, I identified RE-1 consensus sequences in the proximal region of several neuronal specific genes. Chromatin immunoprecipitation (ChIP) assay results have showed that H3K9me2 (dimethylation of lysine 9 on histone 3) occupancy at RE-1 containing sequences from neuronal specific genes was significantly decreased in BIX01294-MSCs. When BIX01294-MSCs were differentiated with neuronal induction medium, cells differentiated more effectively into neuron-like cells

complete with a cell body and dendrites. Expression of neuronal specific genes containing the RE-1 sequences was significantly increased in differentiated BIX01294-MSCs, as confirmed by immunocytochemical staining and immunoblotting. Thus, this study shows that BIX01294-pretreated human BM-MSCs can be effectively differentiated into neuron-like cells by induced expression of neuronal specific genes containing RE-1 sequences. I have further investigated the correlation between protective effect and expression of RE-1 containing neuronal specific genes in G9a inhibited neuronal cells. I have identified the H3K9me2 is increased in hydrogen peroxide (H_2O_2) treated SH-SY5Y cells and that decreased by G9a inhibition. Therefore, I suggest that G9a inhibition was may contribute in treatment of neurodegenerative disorders by oxidative stresses.

국문초록

BIX01294 (G9a inhibitor)를 이용한 신경분화 및 퇴화 제어

현재 연구들은 후생 유전적 변형이 신경분화에 크게 관여한다고 보고된다. 많은 신경특이 유전자들은 repressor element-1 (RE-1)을 포함하고 있고, 이곳에 히스톤 메틸화 효소 G9a와 같은 후생 유전적 조절자들이 결합하여 비 신경세포에서 신경 유전자의 발현을 억제한다. 본 연구에서는 인간 골수 중간엽 줄기세포(BM-MSCs)의 신경분화 동안 G9a의 기능적인 역할을 조사하였다. G9a 억제제 BIX01294가 처리된 인간 골수 중간엽 줄기세포는 다양한 신경계통 유전자의 발현이 증가하는 것이 관찰된다. 본 연구에서 유전자 서열분석을 이용하여 다양한 신경 특이 유전자에서 RE-1 공통서열을 확인하였다. Chromatin immunoprecipitation (ChIP)를 이용하여 신경 특이 유전자의 RE-1을 포함하는 서열에서 H3K9me2의 정도를 확인해본 결과 BIX01294가 처리된 중간엽 줄기세포에서 H3K9me2이 크게 감소되어 있는 것을 확인할 수 있었다. 신경세포 분화 유도 배지에서 BIX01294가 전 처리된 세포가 BIX01294가 전 처리되지 않은 세포보다 신경세포로의 분화가 좀 더 잘 이루어지는 것을 확인하였다. Immunocytochemistry staining 과 immunoblotting을 이용한 RE-1을 포함하는 신경 특이 유전자의 발현분석에서 BIX01294 전 처리 후 분화를 유도한 중간엽 줄기세포가 BIX01294 전 처리 없이 분화를 유도한 중간엽 줄기세포에 비해 RE-1을 포함하는 신경 특이 유전자의 발현이 크게 증가하여 있는 것을 확인하였다. 따라서, 본 연구는 BIX01294가 전 처리된 인간 골수 중간엽 줄기세포가 RE-1을 포함하는 신경 특이 유전자의 발현 유도에 의해 신경세포로의 분화가 촉진되었음을 제시한다. 더 나아가 G9a가 억제된 신경 세포에서 RE-1을 포함하는 신경특이 유전자들의 발현과 보호효과 사이에 연관성을 조사했다. 이 연구에서 과산화수소가 처리된 SH-SY5Y 세포에서 H3K9me2가 증가하는 것을 확인했고 이것은 G9a 억제에 의해 감소된다. 그러므로, G9a 억제는 신경세포에서 산화스트레스에 의해 유도되는 신경세포 손상에서 세포 보호 효과가 있을 것이라고 제안한다.

Part 1. G9a inhibition promotes neuronal differentiation of human bone marrow mesenchymal stem cells through the transcriptional induction of RE-1 containing neuronal specific genes.

1. Introduction

Mesenchymal stem cells (MSCs) are multipotent cells, that can differentiate into diverse cell types, for example osteocytes, chondrocytes, adipocytes, and neuronal cells (Jeong et al., 2013; Pittenger et al., 1999). There is increasing evidence that epigenetic modifications are intimately associated with stem cell differentiation (Hemming et al., 2014; Zhao et al., 2013). Epigenomic changes resulting from the modulation of nuclear histone modifications or DNA methylation lead to neuronal differentiation of human bone marrow MSCs (BM-MSCs) (Jeong et al., 2013; Joe et al., 2015; Oh et al., 2015a; 2015b). However, how epigenomic changes are modulated during neuronal differentiation remains unclear. This study focused on the role of the epigenetic modulator G9a, a histone methyltransferase, during neuronal differentiation of human BM-MSCs.

Many neuronal specific genes contain the consensus sequences of repressor element-1 (RE-1/NRSE) in their proximal region (Bruceet al., 2004; Mortazavi et al., 2006). This element represses gene transcription upon binding to the RE-1 silencing transcription factor (REST/NRSF) in non-neuronal cells (Schoenherr et al., 1996; Thiel et al., 2015). REST contains a DNA binding domain, that recognizes REST binding sequences on genomic DNA, and two repression domains located on the N- and C-termini of REST. The repression domains bind to two co-repressor complexes, mSin3 and CoREST, which recruit histone deacetylases and methyltransferases, respectively, to their

target genes.

Consequently, the recruited enzymes transmute the target genes' chromatin into more tightly packed heterochromatin. Since the latter is inaccessible to transcription enzymes, gene expression is interrupted (Rossbach, 2011; Zheng et al., 2009). G9a histone methyltransferase promotes dimethylation of lysine 9 on histone 3 (H3K9) by transferring a methyl group from S-adenosyl-L-methionine (SAM), thus perturbing DNA transcription (Shankar et al., 2013; Shinkai and Tachibana, 2011). RE-1 bound to REST recruits epigenetic modification enzymes including G9a and represses expression of neuronal specific genes (Ding et al., 2008; 2009).

The non-competitive G9a inhibitor BIX01294 reduces dimethylation (H3K9me2) by blocking the binding of SAM to G9a (Kubicek et al., 2007), consequently increasing gene expression and then used for research of anti-cancer and cell differentiation.

Therefore, this study investigated the role of G9a in neuronal differentiation and found that inhibition of G9a promoted neuronal differentiation via epigenetic modification of neuronal specific genes containing the RE-1 sequences.

ll. Materials and Methods

ll-1. Characteristics of primary human BM-MSCs and cell culture

Human BM-MSCs were purchased from CEFO (Cell Engineering for Origin; Seoul, Korea). The cells tested negative for viral infection and mycoplasma contamination. Flow cytometric analysis of the cells revealed $CD73^{+}$, $CD105^{+}$, and $CD31^{-}$ phenotype. BM-MSCs were cultured in T75 flasks (Becton Dickinson; San Jose, CA, U.S.A.) according the manufacturer's recommendations. Cells were cultured in BM-MSC growth medium (DMEM; Gibco; Grand Island, NY, U.S.A.), containing 10% fetal bovine serum (FBS), L-glutamine, penicillin, and streptomycin, without any stimulatory supplements or vitamins. Cells were maintained in a humidified incubator at 37℃, using a standard mixture of 95% air and 5% CO_2. BM-MSCs at passage seven were used in this study.

ll-2. Real-time PCR

Total RNA was isolated from BM-MSCs using RNAiso reagent (TAKARA; Shiga, Japan) according the manufacturer's instructions. Primescript Ⅱ 1st strand cDNA synthesis kit (TAKARA) was used to reverse transcribe 3-5 μg total RNA with 5 μM Oligo (dT) primers (TAKARA), 1 mM of each dNTP, and the supplied buffer. cDNA was amplified using Power SYBR Green PCR master mix (Applied Biosystems Inc.; U.S.A.) with gene-specific primers for human *Musashi*, *Nestin*, *CD*133, *GFAP*, *MAP*-2, *NF*-M, *Tuj*-1, *KCNH*1, *SYN*1, *SYP*, *SCN*3A, *SNAP*25, *CACNA*1A, *BDNF*,

Adiponectin, *RUNX2*, *Matrilin*-1, *MMP*13, and *β-actin*. The real-time PCR cycling parameters were as follows: 95℃ for 10 min, followed by 40 cycles of 15 s at 95℃, and 1 min at 60℃.

The primers were synthesized by GenoTech (GenoTech Corp.; Daejeon, South Korea) and IDT (Integrated DNA Technologies Inc.; Coralville, IA, U.S.A.) and are summarized in Table 1.

Relative mRNA levels were quantified by $2^{-\triangle\triangle CT}$ methods (Livak and Schmittgen, 2001).

Table 1. Oligonucleotides used for real-time PCR.

Gene	Forward primer (5′ → 3′)	Reverse primer (5′ → 3′)	Acc. No.
Adiponectin	ACATGCCCATTCGCTTTACC	AGAGGCTGACCTTCACATCC	NM_001177800
BDNF	ACCCACACGCTTCTGTATGG	GCAGCCTTCATGCAACCAAA	NM_001143810.1
CACNA1A	CGGCCAGAGTGGCTTACAA	GCTCCTCCCTTGGCAATCTT	NM_023035.2
CD133	CCTGGGGCTGCTGTTTATTAT	ATTTTCCTTCTGTCGCTGGT	NM_006017
GFAP	TGGGAGCTTGATTCTCAGCA	CCTGGGCTTGACCTCTCTGTA	NM_002055
KCNH1	TTGGAGATGTGTTCTGGAAGGAA	AGGGCATCCCGCTTGATC	NM_172362.2
MAP-2	TTGGTGCCGAGTGAGAAGAA	GGTCTGGCAGTGGTTGGTTAA	NM_002374
Matrilin-1	GGTGGGCATTGTCTTCACTG	GGCTCTGAGGCTATTTCCCT	NM_002379
MMP13	TTCCCAGTGGTGGTGATGAA	CAGGATTCCCGCGAGATTTG	NM_002427
Musashi	ATAAAGTGCTGGCGCAATCG	TCGTTCGAGTCACCATCTTGG	NM_002442
Nestin	AGCCCTGACCACTCCAGTTT	GCTGCTTACCACTTTGCCCT	NM_006617
NF-M	GTGAACCACGAGAAGGCTCA	AGGTAGTCTTTGCGCTCCAC	NM_005382
RUNX2	TCTGACCGCCTCAGTGATTT	TGCCTGGGGTCTGTAATCTG	NM_001024630
SCN3A	AACGGATGACCAGGGCAAAT	TCTGAGGGAGACGAGCTTCA	NM_006922.3
SYN1	CCAGCTCAACAAATCCCAGTC	GCGGATGGTCTCAGCTTTCA	NM_006950.3
SYP	TGCCAACAAGACCGAGAGTG	TTCGGCTGACGAGGAGTAGT	NM_003179.2
SNAP25	TCGATCGTGTCGAAGAAGGC	CCGTCCTGATTATTGCCCCA	NM_003081.3
Tuj-1	GGAGATCGTGCACATCCAGG	CGAGGCACGTACTTGTGAGA	NM_006086.3
β-actin	ATCCGCAAAGACCTGTACGC	TCTTCATTGTGCTGGGTGCC	NM_001101

Acc. No, indicates gene access number.

Ⅱ-3. MTT assay

Cell viability of BIX01294-treated MSCs was evaluated using the MTT assay (Sigmae-Aldrich; St. Louis, MO, USA) and was performed according the manufacturer's instructions. Briefly, 2.5×10^3 hBM-MSCs were seeded onto 96-well plates. The next day, the cells were incubated with 0-1.5 μM of BIX01294 for 12 h and subjected to MTT assay.

Ⅱ-4. Immunoblotting

Cells were incubated with 30 ㎕ RIPA buffer containing protease and dephosphatase inhibitors (Santa Cruz Biotechnology; Dallas, Texas, U.S.A.) for 30 min at 4℃ and then centrifuged at 16,000×g for 20 min. Total protein was then subjected to immunoblotting using antibodies against Musashi (1:500), Nestin (1:500), GFAP (1:500), NF-M (1:500), Tuj-1 (1:1000) or β-actin (1:5000; Sigmae-Aldrich), followed by the appropriate horseradish peroxidase-conjugated secondary antibodies (1:10,000; Jackson Immuno Research Laboratories; West Grove, PA, U.S.A.). Antibodies for Musashi, Nestin, GFAP, NF-M and Tuj-1 were purchased from Santa Cruz Biotechnology.

Ⅱ-5. Chromatin immunoprecipitation

BM-MSCs were incubated with/without 1 μM BIX01294 for 12 h H3K9me2-chromatin was purified with an anti-H3K9me2 antibody (Merck; Darmstadt, Germany) using ChIP assay kits (Merck) according the manufacturer's instructions.

Briefly, cells were crosslinked in 1% formaldehyde in growth medium for 10 min at 37℃ and resuspended in 150 ㎕ SDS lysis buffer (1% SDS, 10 mM EDTA, 50 mM Tris, pH 8.1, protease inhibitors). Chromatin was solubilized and sheared by pulsed sonication (Vibra Cell VCX 130; Sonics & Materials Inc; Church Hill, Newtown, U.S.A.). Chromatin containing fractions (supernatant) were diluted 10-fold in Chip dilution buffer (0.01% SDS, 1.1% Triton X-100, 1.2 mM EDTA, 16.7 mM Tris-HCl, pH 8.1, 167 mM NaCl, protease inhibitors), and added to 56 ㎕ protein A-agarose/Salmon sperm DNA for blocking. 4 ㎕ of anti-H3K9me2 antibody was then added, incubated overnight at 4℃ with rotation, subsequently 50 ㎕ protein A-agarose/Salmon sperm DNA were added and incubated for 1 h at 4℃ with rotation. Immune complexes were pelleted by gentle centrifugation and washed with low-salt buffer (0.1% SDS, 1% Triton X-100, 2 mM EDTA, 20 mM Tris-HCl pH 8.1, and 150 mM NaCl), high-salt buffer (0.1% SDS, 1% Triton X-100, 2 mM EDTA, 20 mM Tris-HCl pH 8.1, and 500 mM NaCl), LiCl detergent buffer (0.25M LiCl , 1% IGEPAL-CA630, 1% Deoxycholate, 1 mM EDTA, 10 mM Tris-Cl pH 8.1) and TE buffer. DNA was recovered by elution buffer (1% SDS, 0.1 M $NaHCO_3$) and de-crosslinking at 65℃ for 4 h. Genomic DNA was purified by phenol/chloroform/ethanol precipitation and resuspended in 30 ㎕ distilled water.

Prior to immunoprecipitation, 10% of the chromatin mixture (150 ㎕) was purified and resuspended in 30 ㎕ distilled water as an input control for normalization. For real-time PCR analysis, 3 ㎕ genomic DNA was used for each reaction.

Ⅱ-6. Neuronal differentiation

BM-MSCs were incubated with/without 1 μM BIX01294 for 12 h. The cells were then exposed to pre-induction medium containing DMEM, 10% FBS, 10 ng/ml bFGF, and 500 μM β-mercaptoethanol for 24 h. The medium was replaced with induction medium containing 100 μM butylated hydroxyanisole (BHA) and 2% dimethyl sulfoxide (DMSO) and free of FBS for 6 h, according to previously described procedures (Jeong et al., 2013; Woodbury et al., 2000). Control MSCs were incubated in FBS-containing medium for 24 h. The medium was replaced with FBS-free medium and the cells were further incubated for 6 h. Images were captured with a microscope (Nikon ECLIPSE TS100; Tokyo, Japan) and a digital camera (i-Solution IMTcam3; Tokyo, Japan). Cells were considered differentiated if each cell body had more than two dendrites longer than 60 μm (Jeong et al., 2013). Neurite lengths were measured using ImageJ software (NIH; Bethesda, U.S.A.).

Ⅱ-7. Immunocytochemical staining

BM-MSCs were grown on poly-L-lysine-coated coverslips (Thermo Fisher Scientific; Waltham, MA, U.S.A.) and induced to differentiate into neuron-like cells. Cells were then subjected to immunocytochemical staining with antibodies against Nestin or NF-M (Santa Cruz Biotechnology) diluted 1:200 in blocking buffer overnight at 4℃, followed by Alexa 488-conjugated donkey antigoat IgG secondary antibodies (Thermo Fisher Scientific) diluted 1:500 in Hoechst 33342 (Thermo Fisher Scientific) for 1 h at room temperature.
The cells were visualized using a Nikon Eclipse 80Ti microscope (Nikon). Cell images were taken with a DS-RI1 digital camera (Nikon).

II-8. Statistical analysis

Data are represented as mean ± standard deviation (SD) of three or more independent experiments. Statistical comparisons between groups were made using an independent t-test. A p-value of <0.05 was considered statistically significant.

Ⅲ. Results

Ⅲ-1. Neuroprogenitor genes are induced by BIX01294 in human BMMSCs

To evaluate the effect of BIX01294, BM-MSCs were incubated with 0-1.5 μM of BIX01294 for 12 h. The expression of neuroprogenitor markers, *Musashi* and *Nestin*, was assessed by real-time PCR and immunoblotting. As shown in Fig. 1A, maximum expression was obtained after incubation with 1 μM BIX01294 (Fig. 1A; *t*-test, $^{**}p < 0.005$, mean ± SD, n = 4).

To examine the optimal incubation time with BIX01294, BM-MSCs were treated with 1 μM BIX01294 for several time periods (0-24 h). Expression of the tested genes was maximal after incubation for 12 h (Fig. 1B; *t*-test, $^{**}p < 0.005$, mean ± SD, n = 4). The results were confirmed by immunoblotting with specific antibodies against *Musashi* and *Nestin* (Fig. 1A and B, bottom). Cellular toxicity was not observed in the tested conditions (up to 1.5 μM BIX01294 for 12 h) (Fig. 1C; mean ± SD, n = 3). In summary, it was shown that treatment with 1 μM BIX01294 for 12 h stimulated the expression of neuroprogenitor proteins.

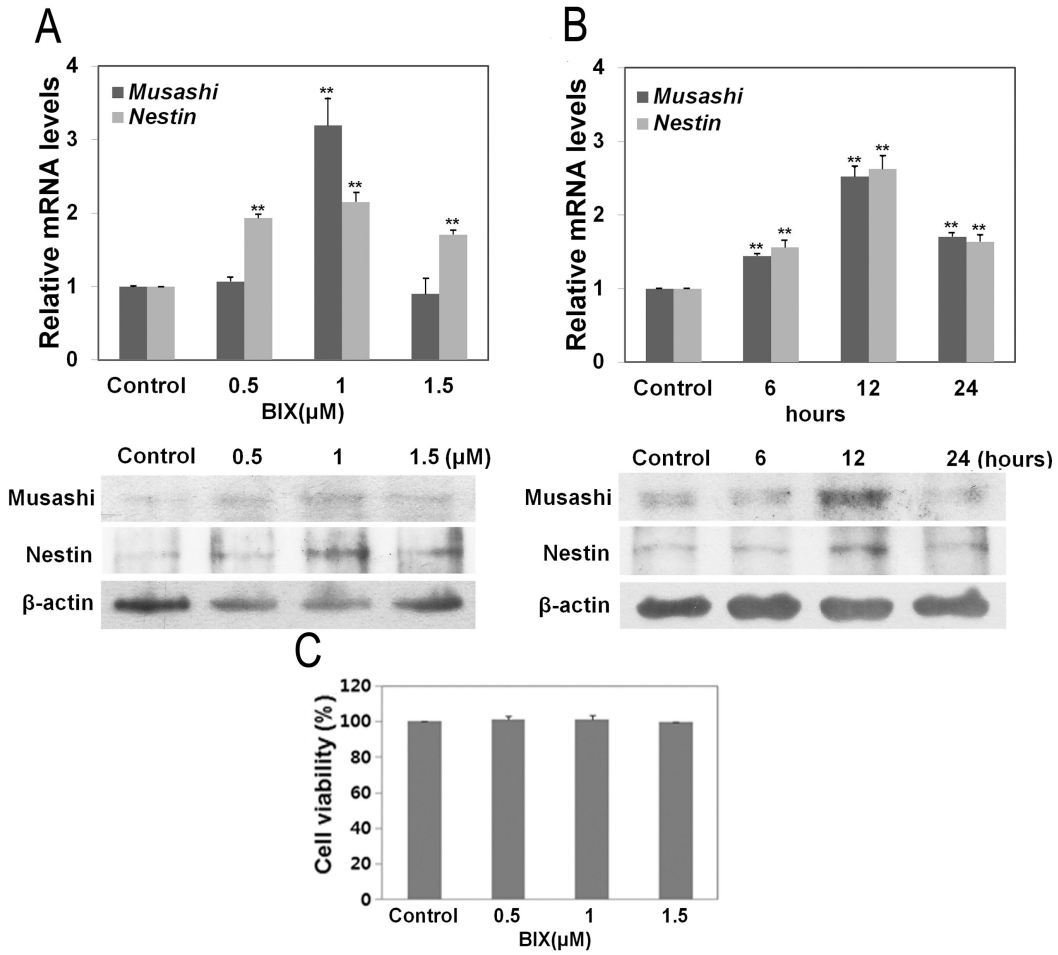

Fig. 1. The expression of neuroprogenitor genes was induced in BIX01294-treated BM-MSCs.

(A) Human BM-MSCs were treated with 0-1.5 μM BIX01294 for 12 h. The expression and protein levels of the neuroprogenitor genes *Musashi* and *Nestin* were measured by real-time PCR and immunoblotting, respectively. (B) 1 μM BIX01294 was applied for several time periods (0-24 h), which expression and protein levels of *Musashi* and *Nestin* were measured by real-time PCR and immunoblotting. (C) No cytotoxicity, measured by MTT assay, was observed under the specified conditions.

III-2. G9a inhibition stimulates the expression of neuronal specific genes containing RE-1 sequences in BM-MSCs

To further investigate the effect of G9a inhibition, MSCs were treated with/without 1 μM BIX01294 for 12 h and then expression of neuronal-lineage genes, *Musashi*, *Nestin*, *CD*133, *GFAP*, *NF*-M, *Syn*1, *SYP*, *SCN*3A, *SNAP*25, *Tuj*-1, and *CACNA*1A was measured by real-time PCR. As shown in Fig. 2A, gene expression was significantly higher in 1 μM BIX01294-treated BM-MSCs (BIX-MSCs) compared to non-treated cells (Ctrl-MSCs) (Fig. 2A; *t*-test, $^{*}p < 0.05$, $^{**}p < 0.005$, mean ± SD, n = 4). I also examined the expression of different lineage specific genes, such as *Adiponectin* (adipocytes); *RUNX*2 (osteocytes); *Matrilin*-1 and *MMP*13 (chondrocytes). The expression of these genes was lower in BIX-MSCs (Fig. 2B; *t*-test, $^{**}p < 0.005$, mean ± SD, n = 4). Immunoblotting was consistent with PCR results, since levels of neuronal specific proteins *Musashi*, *Nestin* and *GFAP* were also higher in BIX-MSCs (Fig. 2C). The H3K9me2 expression was decrease in BIX01294 treated MSCs (data not shown). G9a is an important component of the REST complex (Ooi and Wood, 2007). Using the genomatix software (Cartharius et al., 2005), it was found that many neuronal specific genes contained the RE-1 consensus sequences in the proximal region of their genomic DNA (Table 2).

To examine whether the increased expression of these genes was due to decreased H3K9me2 in the RE-1 sequences found in neuronal specific genes, a chromatin immunoprecipitation (ChIP) assay with an H3K9me2 specific antibody was performed. The H3K9me2 occupancy at RE-1 sequences of neuronal specific genes *Musashi*, *Nestin*, *CD*133, *NF*-M, *Syn*1, and *SNAP*25 was significantly decreased in BIX-MSCs (Fig. 2D).

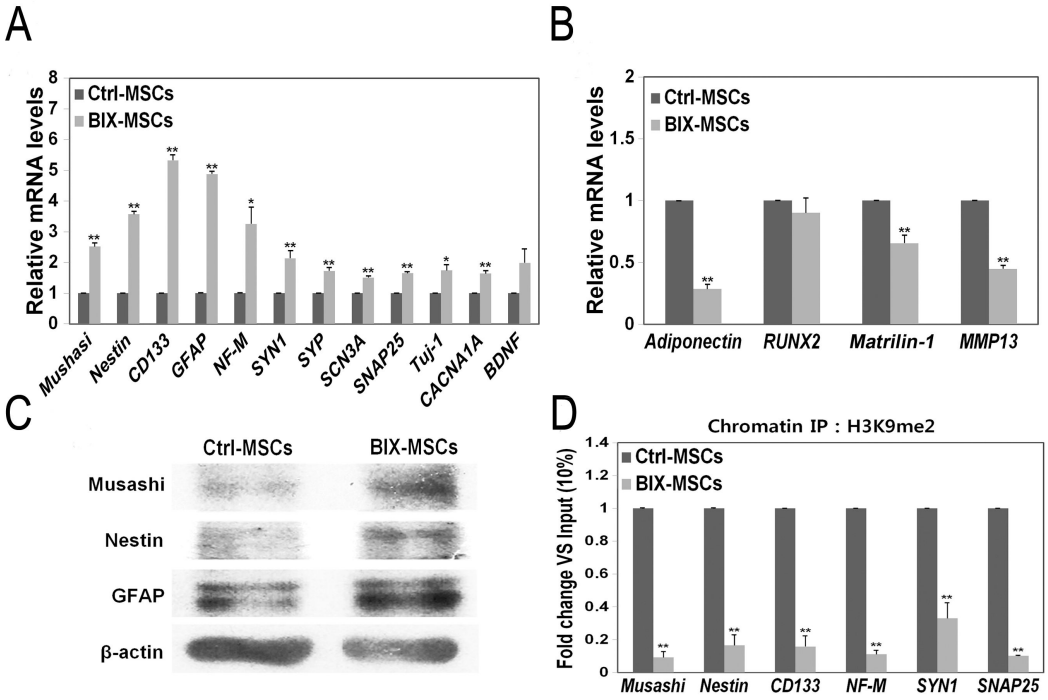

Fig. 2. The RE-1 containing neuronal specific genes are increasingly expressed in BIX-MSCs.

(A) The expression of neuronal specific genes was measured by real-time PCR in non- and BIX01294-treated MSCs (Ctrl- and BIX-MSCs). All genes tested in this experiment, more significantly expressed in BIX-MSCs. (B) The expression of non-neuronal lineage genes was decreased in BIX-MSCs. (C) Neuronal specific proteins were also increased in BIX-MSCs. β-actin was used as a standard control. (D) Soluble chromatin isolated from Ctrl- or BIX-MSCs was immunoprecipitated with the H3K9me2 specific antibody, and then analyzed by real-time PCR using primers flanking RE-1 sequences within the *Nestin*, *CD133*, *NF*-M, *SYN*1, and *SNAP*25 genes.

Table 2. Genes containing the consensus sequences of repressor element-1. Chr indicates chromosome.

Genes	Gene Location	RE-1 Positions on genome
CACNA1A	NC_000019.10	Chr19 : 13,506,365 - 13,506,395
CD133	NC_000004.12	Chr4 : 16,076,172 - 16,076,202
GFAP	NC_000017.11	Chr17 : 44,913,340 - 44,913,370
Musashi	NC_000012.12	Chr12 : 120,366,434 - 120,366,464
Nestin	NC_000001.11	Chr1 : 156,678,984 - 156,679,014
NF-M	NC_000008.11	Chr8 : 24,914,943 - 24,914,973
SNAP25	NC_000020.11	Chr20 : 10,219,672 - 10,219,694
SYN1	NC_000023.11	ChrX : 47,620,070 - 47,620,090
SYP	NC_000023.11	ChrX : 49,200,840 - 49,200,870
Tuj-1	NC_000016.10	Chr16 : 89,923,464 - 89,923,494

Ⅲ-3. BIX01294-pretreated BM-MSCs have a neuronal appearance in neuronal induction medium

Since G9a inhibition by BIX01294 stimulated the expression of neuronal specific genes, it was hypothesized that BIX-MSCs could be more effectively differentiated into neuronal cells than control MSCs (Ctrl-MSCs). To test this hypothesis, Ctrl- and BIX-MSCs were differentiated with neuronal induction medium. Both neuronal differentiated MSCs (Fig. 3A; dMSCs and BIX-dMSCs) exhibited a neuronal morphology, while undifferentiated BM-MSCs (Ctrl-MSCs) and BIX-MSCs showed a flattened and spindle-shaped appearance similar to primary hBM-MSCs (Fig. 3A, Ctrl-MSCs and BIX-MSCs). Assessing the rate of neuronal differentiation in BIXdMSCs and dMSCs, revealed that BIX-dMSCs were significantly more differentiated into neuron-like cells than dMSCs (Fig. 3B and Table 3; t-test, $^{*}p < 0.05$, mean ± SD, n = 3). The average neurite length of dMSCs was also significantly extended in BIX-dMSCs (Fig. 3C and Table 4; t-test, $^{*}p < 0.05$, mean ± SD, n = 3). A significant difference in the number of neurites was not observed between dMSCs and BIX-dMSCs (Fig. 3D and Table 4).

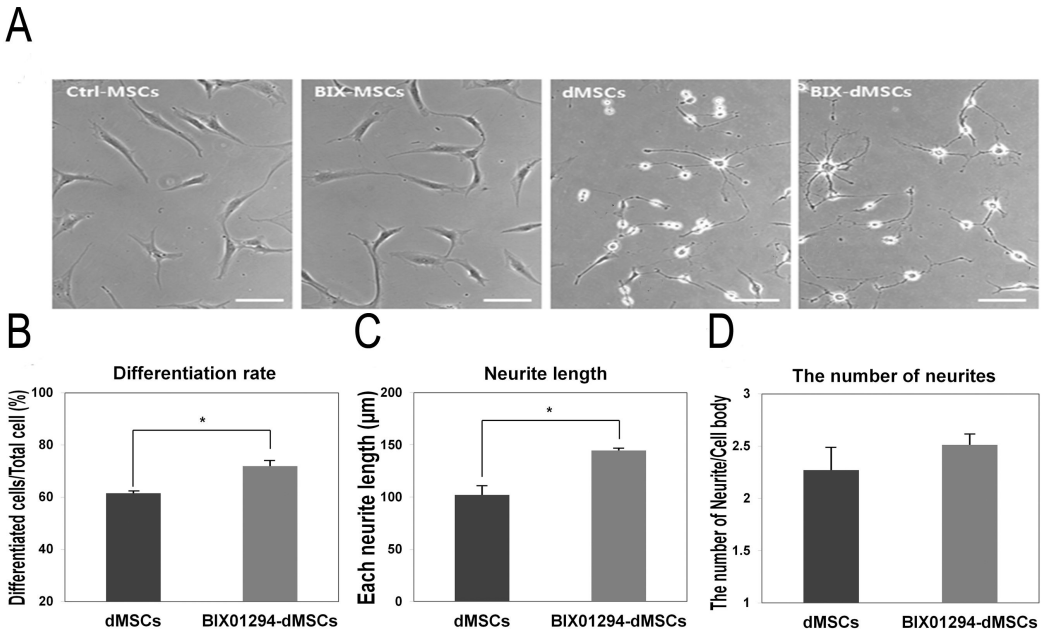

Fig. 3. Neuron-like morphological changes in BIX-MSCs followed by neuronal induction.

(A) Both Ctrl-MSCs and BIX-MSCs differentiated into neuronal cells according exposure to neuronal induction medium. Differentiated MSCs are indicated as dMSCs and BIX-dMSCs. The scale bar indicates 100 μm. (B) Total cells and neuronal shaped cells were counted to estimate the neuronal differentiation rate. BIX-dMSCs were significantly more differentiated compared to dMSCs. (C) The neurite length of differentiated cells was significantly extended in BIX-dMSCs. (D) The number of neurites in differentiated cells did not increase significantly.

Table 3. The neuronal-like cells were counted to estimate the neuronal differentiation rate

Experiments (n=3)	dMSCs (Differentiated cells/total cells)	BIX-dMSCs (Differentiated cells/total cells)
1st	338 / 537	387 / 553
2nd	485 / 802	496 / 710
3rd	339 / 554	437 / 576
Sum	1162 / 1893 (61.4%)	1320 / 1839 (71.8%)

Table 4. The number of neurites from each differentiated cells were counted and neurite lengths were measured.

dMSCs			
Experiments (n=3)	Total cells	The No. of Neurite (Ave/each cell)	Neurite length (Ave/each neurite,㎛)
1st	338	2.13	109.74
2nd	485	1.99	86.23
3rd	339	2.69	110.3
Ave.	387	2.24	102.09

BIX-dMSCs			
Experiments (n=3)	Total cells	The No. of Neurite (Ave/each cell)	Neurite length (Ave/each neurite,㎛)
1st	387	2.34	145.71
2nd	496	2.67	146.51
3rd	437	2.53	141.42
Ave.	440	2.51	144.55

Ⅲ-4. Significantly increased expression of diverse neuronal markers in neuronal differentiated BIX-MSCs

Since BIX-dMSCs displayed a neuronal appearance, the expression of various neuronal specific marker genes was measured by real-time PCR (Fig. 4A). All genes tested in this study were significantly increased in either BIX-dMSCs or dMSCs, compared to undifferentiated MSCs (Ctrl-MSCs) (Fig. 4A; *t*-test, $^{**}p < 0.005$, mean ± SD, n = 4). The expression of neuronal specific marker genes (*Tuj*-1, *MAP*-2, and *KCNH*1) was significantly higher in BIX-dMSCs compared to dMSCs (Fig. 4A; *t*-test, $^{*}p < 0.05$, mean ± SD, n = 4). Expression of other lineage specific markers, such as adipogenic (*Adiponectin*), osteogenic (*RUNX*2), and chondrogenic (*Matrilin*-1, *MMP*13) specific genes, was lower in dMSCs and BIX-dMSCs, compared to Ctrl-MSCs (Fig. 4B; *t*-test, $^{*}p < 0.05$, $^{**}p < 0.005$, mean ± SD, n = 4). To further characterize neuronal differentiated cells at a protein level, immunocytochemical staining was used. Ctrl-MSCs, dMSCs, and BIX-dMSCs were fixed and stained with the neuronal specific proteins Nestin and NF-M. Neuronal differentiated MSCs (dMSCs) and BIX-dMSCs exhibited positive cytoplasmic staining for both Nestin and NF-M, compared to the non-differentiated MSCs (Ctrl-MSCs, Fig. 4C). Consistent results were obtained by immunoblotting using antibodies specific to Nestin and NF-M (Fig. 4D).

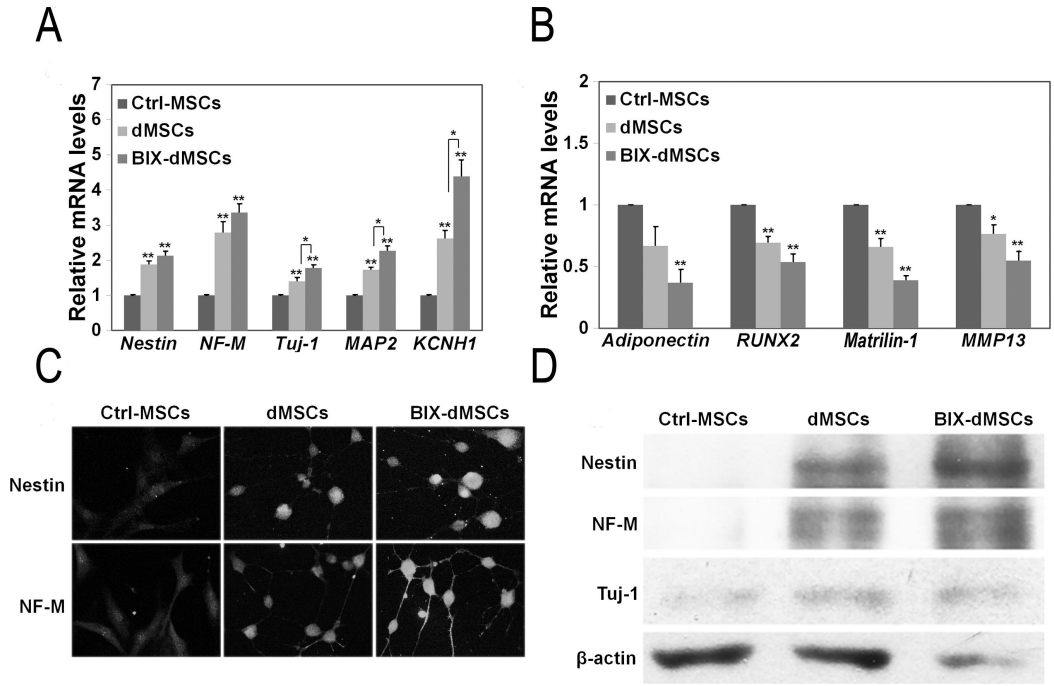

Fig. 4. Increased expression of diverse neuronal markers in differentiated BIX-MSCs.

(A) The expression of neuronal specific genes was analyzed by real-time PCR in MSCs (Ctrl-MSCs) and differentiated MSCs (dMSCs and BIX-dMSCs). All tested genes were significantly increased in both dMSCs. *Tuj*-1, *MAP2*, and *KCNH1* were significantly increased in BIX-dMSCs compared to dMSCs. (B) The expression of osteogenic, adipogenic and chondrogenic specific genes were decreased in both dMSCs and BIX-dMSCs compared to Ctrl-MSCs. (C) MSCs were stained with neuronal specific antibodies for Nestin (upper panel) and NF-M (lower panel), and visualized by fluorescent microscopy. (D) MSCs were subjected to immunoblotting with neuronal specific antibodies for Nestin, NF-M and Tuj-1.

IV. Discussion

Cellular differentiation leads to dramatic changes in cell shape, size, metabolic function, membrane potential, and cellular signaling (Slack, 2007). These changes are associated with epigenetic modifications that alter gene expression (Hemming et al., 2014; Jeong et al., 2013; Joe et al., 2015; Oh et al., 2015a, 2015b; Zhao et al., 2013), resulting in different physical and functional characteristics in spite of maintaining the same genome. If these changes fail to occur, cells may die or be transformed, as reported during in vitro neuronal differentiation. Thus, epigenomic modulations such as DNA methylation and histone modification play an important role in the transcriptional transitions of many neuronal specific genes during neuronal differentiation (Balasubramaniyan et al., 2006; Ballas and Mandel, 2005).

Previous studies have shown that HDAC or DNMT inhibition effectively stimulates neuronal differentiation (Jeong et al., 2013; Oh et al., 2015b) whether expression of neuronal specific genes resumed according G9a inhibition. To test this hypothesis, the G9a non-competitive inhibitor BIX01294 was used in BM-MSCs, resulting in increased expressions of various neuronal specific genes and the decrease of other lineage specific genes (Fig. 1 and Fig. 2A-C). ChIP assays confirmed that the increased expression was due to decreased H3K9me2 on the RE-1 sequences found in neuronal specific genes (Fig. 2D). Since G9a inhibition stimulated expression of neuronal specific genes in BM-MSCs, it was speculated that BIX01294 treatment may enhance differentiation of neuronal cells. To test this hypothesis, BM-MSCs were induced to differentiate into neuron-like cells in the presence of neuronal induction medium (Jeong et al., 2013; Woodbury et al., 2000). As expected, BIX01294-treated MSCs showed a greater ability to differentiate into neuronal cells (Fig. 3A and B). The differentiated cells possessed a neuronal appearance, including neurite extensions and a cell body (Fig. 3).

The expression of neuronal specific genes was significantly increased in these cells, whereas other lineage genes were decreased (Fig. 4), suggesting that BIX01294-pretreatment altered gene expression and caused a more effective differentiation into neuronal cells.

Part ll. G9a inhibition prevents neuronal death caused by oxidative stress in human neuroblastoma cells.

1. Introduction

Neurodegenerative diseases were associated with neuronal cell death induced by the diverse abnormal factors for example, hypoxia, inflammation, Amyloid β, ethanol (Kauser et al., 2016; Olney et al., 2002; Ramesh et al., 2015; Wang et al., 2016). Recent studies have shown that abnormal epigenetic changes play an important role in progression of neuronal degeneration (Noh et al., 2012). They provided the evident that neuron degeneration were caused through epigenetic changes stimulated by hypoxia and ethanol (Liu and Le., 2014; Subbanna et al., 2014). Thus, maintaining of epigenetic pattern in neuronal cells are important for preventing the neurodegenerative diseases. Histone methyltransferase G9a is a component of REST (RE-1 silencing transcription factor) complex, which binds to RE-1 (repressor element-1) consensus sequence (Thiel et al., 2015; Zheng et al., 2009). The bound G9a to the RE-1 region is leaded to dimethylation of the 9 lysine residue on histone 3 (H3K9me2) which is associated with repression of RE-1 containing neuronal specific genes (Ding et al., 2009; Ding et al., 2008). Unexpected activation of G9a by hypoxia or ethanol increases the risk of neurodegeneration (Subbanna et al., 2013; Wang et al., 2011). G9a inhibition using the specific inhibitor such as BIX01294 has beneficial effect on antisenescence (Ahn et al., 2016) and promotes neuronal differentiation of mesenchymal stem cells (Kim et al., 2016) suggests that G9a inhibition may have positive influence in degenerative disorders. BIX01294 a non-competitive selective G9a inhibitor has been used in G9a inhibition studies. In this study, I examine the role of G9a using the inhibitor BIX01294 in oxidative stress induced neuronal cells.

ll. Materials and Methods

ll-1. Cell culture

Human neuroblastoma cell line SH-SY5Y cells were purchased from KCLB (Korean Cell Line Bank; Seoul, Korea). SH-SY5Y cells were cultured in 100mm dish (SPL; pocheon, Gyeonggi-do, Korea.) according the manufacturer's recommendations. Cells were cultured in DMEM/F12 (WELLGENE; Deagu, Korea.) containing 10% fetal bovine serum (FBS), HEPES, sodium bicarbonate, L-glutamine, penicillin, and streptomycin, without any stimulatory supplements or vitamins. Cells were maintained in a humidified incubator at 37°C, using a standard mixture of 95% air and 5% CO_2.

ll-2. MTT assay

Cell viability of BIX01294-treated cells was evaluated using the MTT assay (Sigma-Aldrich; St. Louis, MO, USA) according to the manufacturer's instructions. Briefly, 2×10^3 SH-SY5Ys were seeded onto 96-well plates. The next day, cells were incubated with 0 - 2 μM of BIX01294 for 12 h or expose to H_2O_2, and then subjected to MTT assay.

II-3. Real-time PCR

Total RNA was isolated from SH-SY5Y cells using RNAiso reagent (TAKARA; Shiga, Japan) according the manufacturer's instructions. 3 μg total RNA was used to reverse transcribe using AMPIGENE® cDNA synthesis kit (Enzo; Executive Blvd, Farmingdale, NY, U.S.A.). cDNA was amplified using Power SYBR Green PCR master mix (Applied Biosystems Inc.; U.S.A.) with gene-specific primers for human *MAP*-2, *NF*-M, *NEFH*, *SYN*1, *SCN*3A, *SNAP*25, *CACNA*1A, and *β-actin*. The real-time PCR cycling parameters were as follows: 95°C for 10 min, followed by 40 cycles of 15 s at 95°C, and 1 min at 60°C. The primers used in this study were synthesized by GenoTech (GenoTech Corp; Daejeon, South Korea) and IDT (Integrated DNA Technologies Inc; Coralville, IA, U.S.A.) and are summarized in Table 1.

Table 1. Oligonucleotides used for real-time PCR.

Gene	Forward primer (5′ → 3′)	Reverse primer (5′ → 3′)	Acc. No.
NF-M	ATAAAGTGCTGGCGCAATCG	TCGTTCGAGTCACCATCTTGG	NM_002442
NEFH	AGCCCTGACCACTCCAGTTT	GCTGCTTACCACTTTGCCCT	NM_006617
MAP2	CCTGGGGCTGCTGTTTATTAT	ATTTTCCTTCTGTCGCTGGT	NM_006017
SCN3A	TGGGAGCTTGATTCTCAGCA	CCTGGGCTTGACCTCTCTGTA	NM_002055
CACNA1A	TTGGTGCCGAGTGAGAAGAA	GGTCTGGCAGTGGTTGGTTAA	NM_002374
SYN1	GTGAACCACGAGAAGGCTCA	AGGTAGTCTTTGCGCTCCAC	NM_005382
SNAP25	TTGGAGATGTGTTCTGGAAGGAA	AGGGCATCCCGCTTGATC	NM_172362.2
β-actin	ATCCGCAAAGACCTGTACGC	TCTTCATTGTGCTGGGTGCC	NM_001101

Acc. No, indicates gene access number.

Ⅱ-4. Immunoblotting

Cells were incubated with 100 ㎕ RIPA buffer containing protease and dephosphatase inhibitors (Santa Cruz Biotechnology; Dallas, Texas, U.S.A.) for 30 min at 4°C and then centrifuged at 16,000×g for 20 min. Total protein was then subjected to immunoblotting using antibodies against Nestin (1:500), NF-M (1:500), MAP-2 (1:500) or β-actin (1:5000; Sigma-Aldrich), followed by the appropriate horseradish peroxidase-conjugated secondary antibodies (1:10,000; Jackson ImmunoResearch Laboratories; West Grove, PA, U.S.A.). Antibodies for Nestin, NF-M and MAP-2 were purchased from Santa Cruz Biotechnology.

Ⅱ- 5. ChIP assay

Cells were incubated with/without 1 μM BIX01294 for 12 h and then treated with 100 μM H_2O_2 for 12 h. H3K9me2 containing chromatins were precipitated by an anti-H3K9me2 antibody (Merck; Darmstadt, Germany) and subjected to ChIP using the ChIP assay kits (Merck; Darmstadt, Germany) according the manufacturer's instructions. Prior to immunoprecipitation, 10% of the chromatin mixture (150 ㎕) was purified the genomic DNA and resuspended in 30 ㎕ distilled water as an input control for normalization. For real-time PCR analysis, 3 ㎕ DNA was used for each reaction. The detail method was described in previous studies (Kim et al., 2016).

Ⅱ-6. Neuronal differentiation

SH-SY5Y cells were incubated with/without 1 μM BIX01294 for 12 h. Next, cells were washed with PBS and treated with 50 μM H_2O_2 for 12 h. The cells were washed twice with PBS and replaced to neuronal induction medium containing DMEM-F12, 0.1% FBS, 1 μM retinoic acid for 3-7 days. Control SH-SY5Y cells were incubated in 10% FBS medium for 3 days. Images were captured with a digital camera (i-Solution IMTcam3; Tokyo, Japan) under a microscope (Nikon ECLIPSE TS100; Tokyo, Japan).

Ⅱ-7. Statistical analysis

Data are represented as mean ± standard deviation (SD) of three or more independent experiments. Statistical comparisons between groups were made using an independent t-test. A p-value of < 0.05 was considered statistically significant.

Ⅲ. Result

Ⅲ-1. BIX01294 has the protective effects on apoptosis by oxidative stress in neural cells.

To examine the toxicity of BIX01294, SH-SY5Y cells were incubated with 0 - 2 μM of BIX01294 for 12 h. Cell viability was approximately 10% decreased in BIX01294 2 μM treated cells but other concentrations were not toxic on the cells (Fig. 1A; *t*-test, $^{*}p < 0.05$, mean ± SD, $n = 3$). To identify the cell death by H_2O_2, SH-SY5Y cells were treated with 0-100 μM H_2O_2 for 12 h. The cell survival rate was decreased as dose dependent manner in H_2O_2 treated cells (Fig. 1B; *t*-test, $^{*}p < 0.05$, $^{**}p < 0.005$, mean ± SD, $n = 3$). To evaluate the optimal conditions on protective effect of BIX01294, SH-SY5Y cells were treated with/without BIX01294 as several concentrations and several time points prior to expose 100 μM H_2O_2. The optimal condition of BIX01294 against H_2O_2-induced cell death was 1 μM and 12 h (Fig. 1C-D; *t*-test, $^{\#}p$, $^{*}p < 0.05$, $^{\#\#}p$, $^{**}p < 0.005$, mean ± SD, $n = 3$). In this condition, I confirmed the apoptotic markers caspase 3 and cleaved caspase 3. Caspase 3 was decreased in H_2O_2 treated cells and cleaved caspase 3 were increased in H_2O_2 treated cells (Fig. 1E).

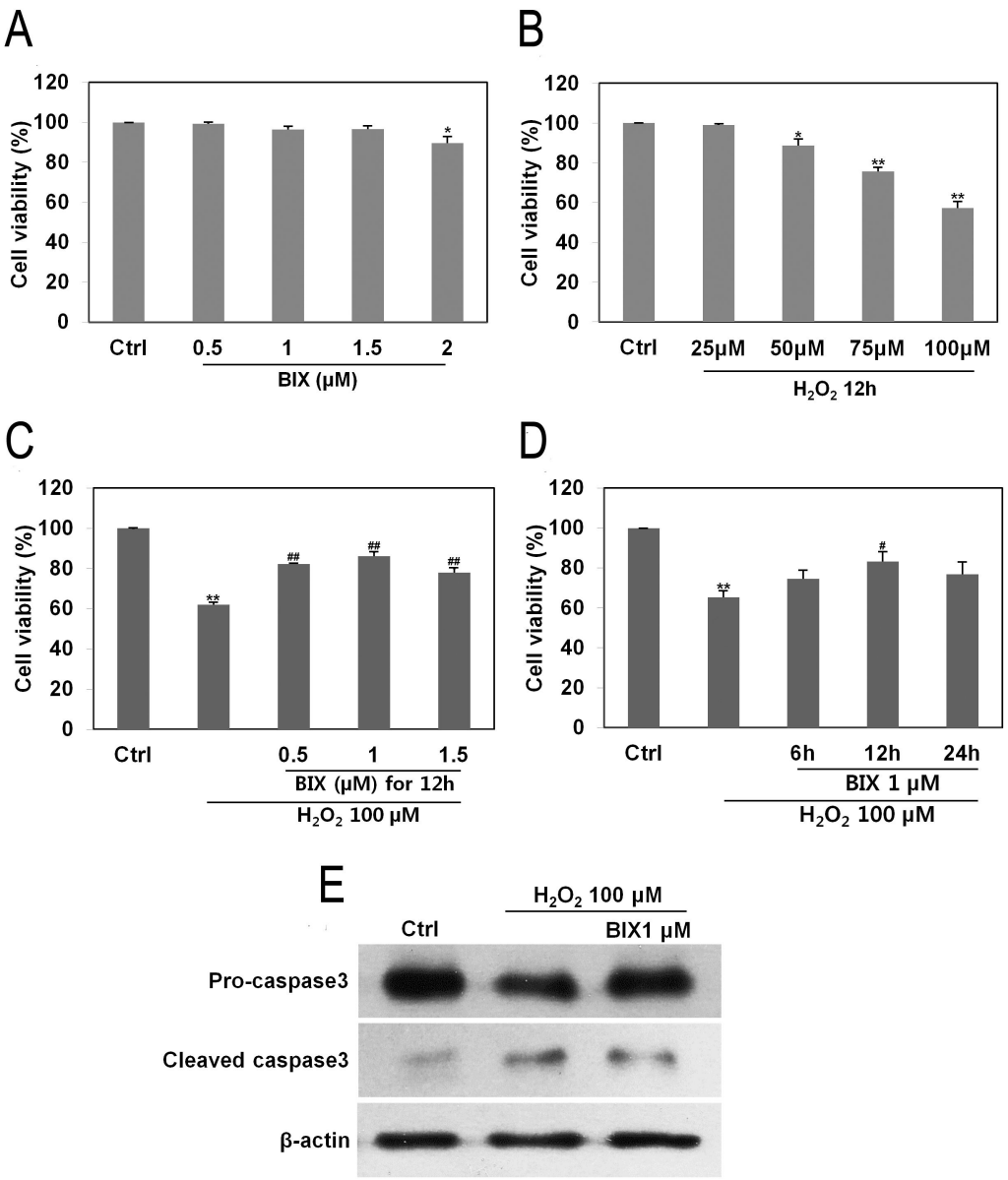

Fig 1. Protective effects of BIX01294 in oxidative damaged neuronal cells.

(A) Toxicity was measured by MTT assay in 0-2 μM BIX01294 treated SH-SY5Y cells. (B) Cells were treated with 0-100 μM H_2O_2 for 12 h. (C) Cells were incubated with 0-1.5 μM BIX01294 and then treated with/without 100 μM H_2O_2. (D) Cells were treated with 1 μM BIX01294 for 0-24 h and then treated with/without 100 μM H_2O_2 for 12 h. (E) Immunoblot analysis was performed with specific antibodies for caspase-3 and cleaved caspase-3 in H_2O_2 or BIX01294 treated cells. $^{*}p$, $^{**}p$ (versus control), $^{\#}p$, $^{\#\#}p$ (versus H_2O_2 100 μM treated cells).

III-2. Downregulation of RE-1 containing neuronal genes by oxidative stress was caused by the activation of G9a.

To further investigate the H_2O_2 mediated neuronal cell damage, SH-SY5Y cells were treated with/without 1 μM BIX01294 for 12 h and then treated with 100 μM H_2O_2 for 12 h. Total RNA were measured by real-time PCR with neuronal specific genes, *NF*-M, *NEFH*, *MAP*-2, *SCN*3A, *CACNA*1A, *Syn*1, and *SNAP*25. As shown in Fig 2A, the tested gene expressions were decreased in H_2O_2 treated cells, then significantly increased by BIX01294 treatmet (Fig. 2A; *t*-test, $^{\#}p$, $^{*}p < 0.05$, $^{\#\#}p$, $^{**}p < 0.005$, mean ± SD, $n = 4$). I also observed them on the protein levels. The neuronal specific proteins, Nestin, NF-M and MAP-2 were also decreased by H_2O_2 treated cells and then recovered in BIX01294-treatment (Fig. 2B). To examine the relationship between oxidative stress and G9a, I examined the G9a activity performing immunoblot analysis with specific antibody for histone 3 lysine 9 dimethylation (H3K9me2). The H3K9me2 (reflect G9a activity) was 1.8-fold increased in H_2O_2 treated cells compared non-treated cells, and 1.5-fold decreased in BIX01294-treatment. Fold change were measured by image j software (Fig. 2C; *t*-test, $^{*}p < 0.05$, mean ± SD, $n = 4$). Furthermore, H3K9me2 occupancy in RE-1 site of neuronal specific genes was significantly increased by H_2O_2 and reduced by BIX01294, examined by ChIP assay (Fig. 2D; *t*-test, $^{*}p < 0.05$, mean ± SD, $n = 3$). These results indicated the G9a inhibition protects against oxidative damage and neuronal degeneration.

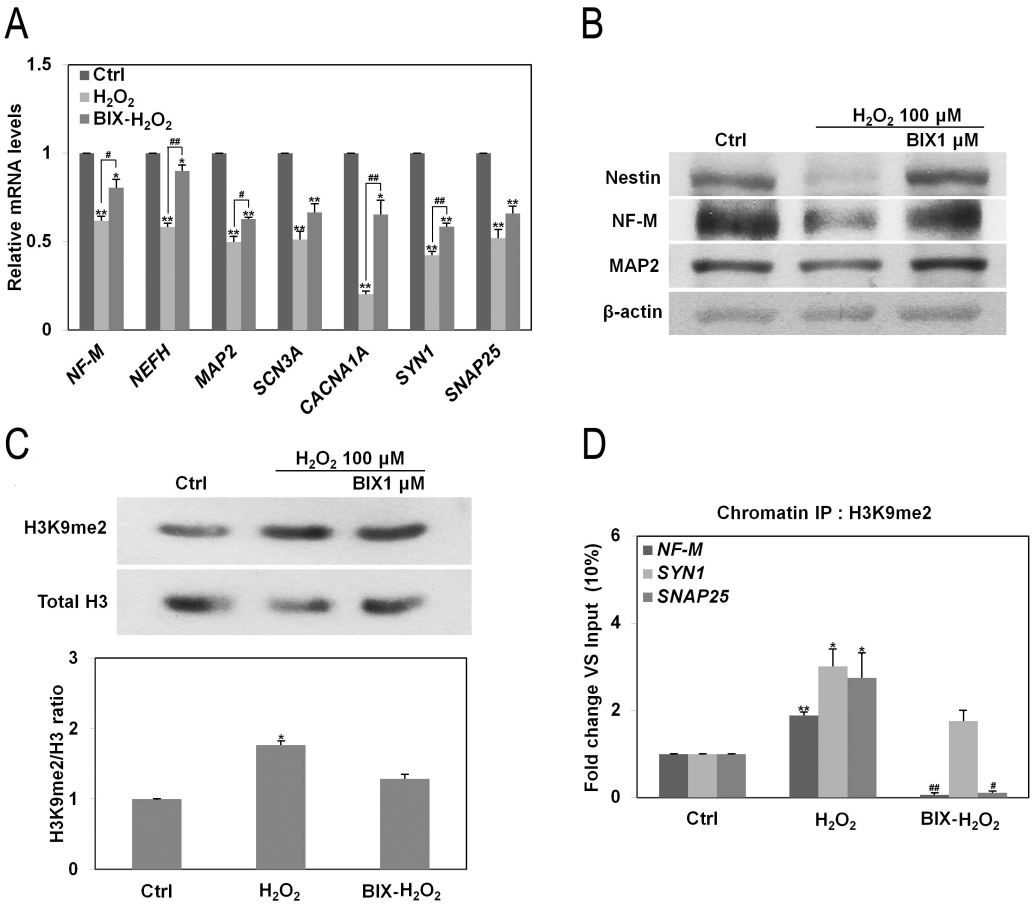

Fig 2. G9a inhibition was against H_2O_2 - induced decrease of neuronal specific genes.

(A) Expressions of Neuronal specific genes were compared with normal condition (Ctrl), H_2O_2-treated cells and BIX01294 treated H_2O_2-cells, which were measured by Real-time PCR. (B) The neuronal specific proteins Nestin, NF-M and MAP-2 were examined by immunoblot analysis in H_2O_2 or BIX treated cells. (C) G9a activity were measured by immunobolt analysis with specific antibody for H3K9me2. (D) For ChIP assay, cells treated with H_2O_2 or BIX were immunoprecipitated with H3K9me2 specific antibody, and then measured by real-time PCR using primers designed around RE-1 site of *NF*-M, *SYN*1, or *SNAP*25 genes. Normal condition (Ctrl), H_2O_2-treated cells (H_2O_2), BIX01294 pre-treated and H_2O_2-treated cells (BIX-H_2O_2). $^{*}p$, $^{**}p$ (versus control), $^{\#}p$, $^{\#\#}p$ (versus H_2O_2 100 μM treated cells).

III-3. G9a inhibition prevented the neuronal cell dysfunction by H_2O_2.

To investigate the functional recovery of H_2O_2 damaged cells by G9a inhibition, SH-SY5Y cells were incubated with/without BIX01294 prior to expose H_2O_2. The cells were induced neuronal differentiation with induction medium. As shown in Fig 3A, differentiation rates were declined in H_2O_2 treated cells (HdSH-SY5Y), and partially recovered with BIX01294 treated cells (BHdSH-SY5Y) (Fig. 3A). To further confirm this data, immunoblot analysis were performed with neuronal specific antibodies, NF-M and MAP2. The protein levels of neuronal genes were decreased in H_2O_2 treated cells, and increased by BIX01294-treatment (Fig. 3B).

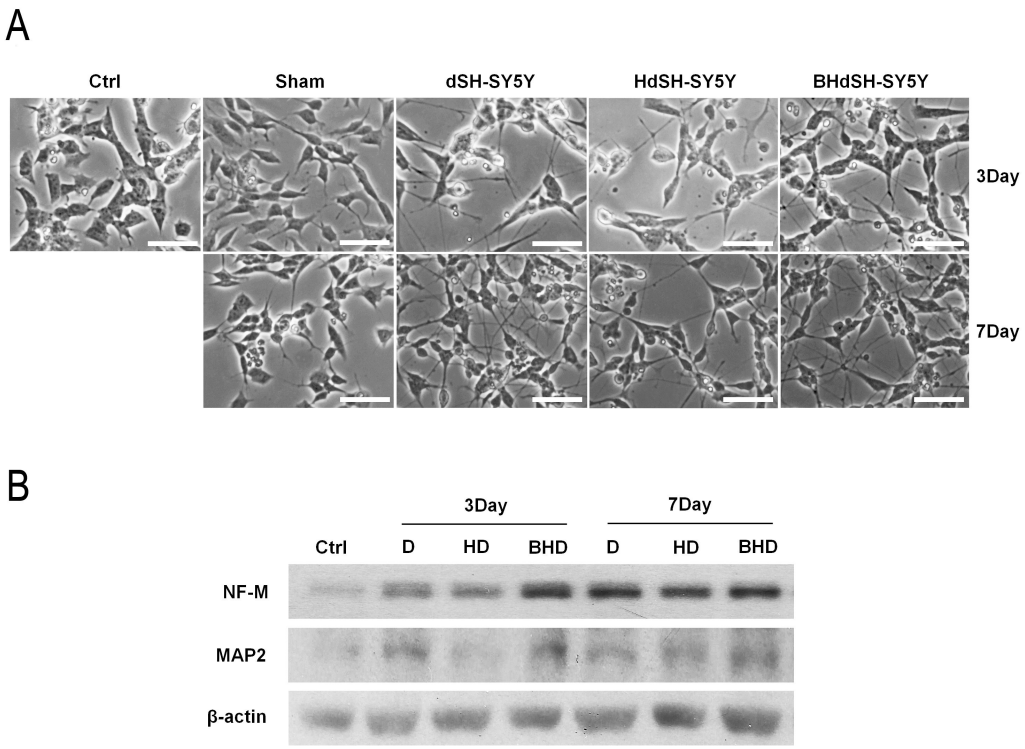

Fig 3. Decline of neuronal differentiation in H_2O_2 treated SH-SY5Y cells and recovery by G9a inhibition.

(A) SH-SY5Y cells were induced to differentiate into neuron like cells for 0-7 days. Each cells was visualized under a light microscopy. The scale bar indicates 100 μm. (B) RE-1 containing neuronal specific genes expressions were examined with specific antibodies for NF-M and MAP-2 in H_2O_2 or BIX treated differentiated SH-SY5Y cells. Non-differentiated cells (Ctrl), FBS 0.1% medium (Sham), normal condition differentiated (dSH-SY5Y or D), H_2O_2-treated differentiated (HdSH-SY5Y or HD), BIX01294 pre-treated and H_2O_2-treated differentiated (BHdSH-SY5Y or BHD).

IV. Discussion

The epigenetic modifications were associated with neuronal differentiation and also paradoxically with neuronal degeneration (Chen et al., 2014; Schweizer et al., 2015; Zhou et al., 2016). Previous studies have shown that a modulation of histone methylation, acetylation and DNA methylation stimulates the expression of neuronal specific genes as result in promoting neuronal differentiation (Jeong et al., 2013; Joe et al., 2015; Kim et al., 2016; Oh et al., 2016). It has been known that histone methyltransferase G9a regulates the expression of RE-1 containing neuronal specific genes through binding to REST complex (Roopra et al., 2004), and activation of G9a by several stimulate such as ethanol and hypoxia was lead to neurodegeneration (Subbanna and Basavarajappa, 2014; Wang et al., 2011). Thus, restrain of over-activated G9a is important in preventing the neurodegenerative disease. In this study I investigated the relationship between neuronal cell death and G9a which induced by oxidative stress in SH-SY5Y cells. As shown in Fig. 1B, cell viabilities were decreased in H_2O_2 treated SH-SY5Y cells, which were accompanied with decreasing the expression of neuronal specific genes (Fig. 2A and Fig. 2B). These declines were prevented by treatment of G9a inhibitor BIX01294 (Fig. 1C-1D and Fig. 2A-2B). These data indicate that the expression of neuronal genes may be disturbed by stress induced G9a activation, and that lead to neuronal cell death.

From ChIP assay, H3K9me2 in H_2O_2-cells were significantly increased in proximal region of RE-1 containing neuronal specific genes compared to control (Fig. 2D), while decreased in BIX treated H_2O_2-cells. When the activation of G9a interrupts neuronal differentiation and lead to neurodegeneration, I examined the neuronal differentiation potency using SH-SY5Y cells which were treated with/without BIX01294 prior to H_2O_2 expose. The neuronal differentiation rate was decreased in H_2O_2 expose

SH-SY5Y cells and that prevented by G9a inhibition (Fig. 3A and Fig. 3B). In summary, hydrogen peroxide were occurrence the cell death and repress of neuronal specific genes by activation of G9a in SH-SY5Y cells, also that related with neurodegeneration. It is significantly recovery by G9a inhibition. This suggests that G9a inhibition may contribute in treatment of neurodegenerative diseases which were caused by oxidative stress.

CONCLUSION

The present study investigated the role of G9a in neuronal differentiation and neuronal degeneration. Using the G9a specific inhibitor BIX01294, it was shown that BIX-MSCs induced the expression of neuronal specific genes, by promoting the transition into an open chromatin form of RE-1 containing sequences. In addition, it was shown that G9a inhibition promoted neuronal differentiation in BM-MSCs. This suggests that resuming the expression of neuronal genes is required during neuronal differentiation and that the histone modification protein G9a may play a role in this process. Moreover, abnormal activation of G9a by hydrogen peroxide were lead to neuronal cell death and repression of neuronal specific genes in SH-SY5Y cells, that recovery by BIX01294-treatment. The differentiation rate of SH-SY5Y cells was also decreased in H_2O_2 treated cells and recovered by BIX01294-treatment. Thus, using a BIX01294 such as G9a inhibitor may provide a better strategy for neuronal differentiation of stem cells and prevent the neurodegeneration.

REFERENCES

Ahn, M.J., Jeong, S.G., Cho, G.W., 2016. Antisenescence activity of G9a inhibitor BIX01294 on human bone marrow mesenchymal stromal cells. Turk J Biol 40, 443-451.

Balasubramaniyan, V., Boddeke, E., Bakels, R., Kust, B., Kooistra, S., Veneman, A., Copray, S., 2006. Effects of histone deacetylation inhibition on neuronal differentiation of embryonic mouse neural stem cells. Neuroscience 143, 939-951.

Ballas, N., Mandel, G., 2005. The many faces of REST oversee epigenetic programming of neuronal genes. Curr. Opin. Neurobiol. 15, 500-506.

Bruce, A.W., Donaldson, I.J., Wood, I.C., Yerbury, S.A., Sadowski, M.I., Chapman, M., Gottgens, B., Buckley, N.J., 2004. Genome-wide analysis of repressor element 1 silencing transcription factor/neuron-restrictive silencing factor (REST/NRSF) target genes. Proc. Natl. Acad. Sci. U. S. A. 101, 10458-10463.

Cartharius, K., Frech, K., Grote, K., Klocke, B., Haltmeier, M., Klingenhoff, A., Frisch, M., Bayerlein, M., Werner, T., 2005. MatInspector and beyond: promoter analysis based on transcription factor binding sites. Bioinformatics 21, 2933-2942.

Chen, X., Du, Z., Shi, W., Wang, C., Yang, Y., Wang, F., Yao, Y., He, K., Hao, A., 2014. 2-Bromopalmitate modulates neuronal differentiation through the regulation of histone acetylation. Stem Cell Res 12, 481-491.

Coulson, J.M., 2005. Transcriptional regulation: cancer, neurons and the REST. Curr. Biol. 15. R665-R658.

Ding, N., Tomomori-Sato, C., Sato, S., Conaway, R.C., Conaway, J.W., Boyer, T.G., 2009. MED19 and MED26 are synergistic functional targets of the RE1 silencing transcription factor in epigenetic silencing of neuronal gene expression. J. Biol. Chem. 284, 2648-2656.

Ding, N., Zhou, H., Esteve, P.O., Chin, H.G., Kim, S., Xu, X., Joseph, S.M., Friez, M.J., Schwartz, C.E., Pradhan, S., Boyer, T.G., 2008. Mediator links epigenetic silencing of neuronal gene expression with x-linked mental retardation. Mol. Cell. 31, 347-359.

Hemming, S., Cakouros, D., Isenmann, S., Cooper, L., Menicanin, D., Zannettino, A., Gronthos, S., 2014. EZH2 and KDM6A act as an epigenetic switch to regulate mesenchymal stem cell lineage specification. Stem Cells 32, 802-815.

Jeong, S.G., Ohn, T., Kim, S.H., Cho, G.W., 2013. Valproic acid promotes neuronal differentiation by induction of neuroprogenitors in human bone-marrow mesenchymal stromal cells. Neurosci. Lett. 554, 22-27.

Joe, I.S., Jeong, S.G., Cho, G.W., 2015. Resveratrol-induced SIRT1 activation promotes neuronal differentiation of human bone marrow mesenchymal stem cells. Neurosci. Lett. 584, 97-102.

Kauser, H., Sahu, S., Panjwani, U., 2016. Guanfacine promotes neuronal survival in medial prefrontal cortex under hypobaric hypoxia. Brain Res 1636, 152-160.

Kim, H.T., Jeong, S.G., Cho, G.W., 2016. G9a inhibition promotes neuronal differentiation of human bone marrow mesenchymal stem cells through the transcriptional induction of RE-1 containing neuronal specific genes. Neurochem Int 96, 77-83.

Kubicek, S., O'Sullivan, R.J., August, E.M., Hickey, E.R., Zhang, Q., Teodoro, M.L., Rea, S., Mechtler, K., Kowalski, J.A., Homon, C.A., Kelly, T.A., Jenuwein, T., 2007. Reversal of H3K9me2 by a small-molecule inhibitor for the G9a histone methyltransferase. Mol. Cell. 25, 473-481.

Liu, H., Le, W., 2014. Epigenetic modifications of chronic hypoxia-mediated neurodegeneration in Alzheimer's disease. Transl Neurodegener 3, 7.

Livak, K.J., Schmittgen, T.D., 2001. Analysis of relative gene expression data using real-time quantitative PCR and the $2^{-\triangle\triangle CT}$ method. Methods 25,

402-408.

Mortazavi, A., Leeper Thompson, E.C., Garcia, S.T., Myers, R.M., Wold, B., 2006. Comparative genomics modeling of the NRSF/REST repressor network: from single conserved sites to genome-wide repertoire. Genome Res. 16, 1208-1221.

Noh, K.M., Hwang, J.Y., Follenzi, A., Athanasiadou, R., Miyawaki, T., Greally, J.M., Bennett, M.V., Zukin, R.S., 2012. Repressor element-1 silencing transcription factor (REST)-dependent epigenetic remodeling is critical to ischemia-induced neuronal death. Proc Natl Acad Sci U S A 109, E962-971.

Oh, Y.S., Jeong, S.G., Cho, G.W., 2015a. Anti-senescence effects of DNA methyltransferase inhibitor RG108 in human bone marrow mesenchymal stromal cells. Biotechnol. Appl. Biochem. 62, 583-590.

Oh, Y.S., Kim, S.H., Cho, G.W., 2015b. Functional restoration of amyotrophic lateral sclerosis patient-derived mesenchymal stromal cells through inhibition of DNA methyltransferase. Cell. Mol. Neurobiol 36, 613-620.

Olney, J.W., Tenkova, T., Dikranian, K., Qin, Y.Q., Labruyere, J., Ikonomidou, C., 2002. Ethanol-induced apoptotic neurodegeneration in the developing C57BL/6 mouse brain. Brain Res Dev Brain Res 133, 115-126.

Ooi, L., Wood, I.C., 2007. Chromatin crosstalk in development and disease: lessons from REST. Nat. Rev. Genet. 8, 544-554.

Pittenger, M.F., Mackay, A.M., Beck, S.C., Jaiswal, R.K., Douglas, R., Mosca, J.D., Moorman, M.A., Simonetti, D.W., Craig, S., Marshak, D.R., 1999. Multilineage potential of adult human mesenchymal stem cells. Science 284, 143-147.

Ramesh, G., Meisner, O.C., Philipp, M.T., 2015. Anti-inflammatory effects of dexamethasone and meloxicam on Borrelia burgdorferi-induced inflammation in neuronal cultures of dorsal root ganglia and myelinating cells of the peripheral nervous system. J Neuroinflammation 12, 240.

Roopra, A., Qazi, R., Schoenike, B., Daley, T.J., Morrison, J.F., 2004. Localized domains of G9a-mediated histone methylation are required for silencing of

neuronal genes. Mol. Cell 14, 727-738.

Rossbach, M., 2011. Non-coding RNAs in neural networks, REST-assured. Front. Genet. 2, 8.

Schoenherr, C.J., Paquette, A.J., Anderson, D.J., 1996. Identification of potential target genes for the neuron-restrictive silencer factor. Proc. Natl. Acad. Sci. U. S. A. 93, 9881-9886.

Schweizer, S., Harms, C., Lerch, H., Flynn, J., Hecht, J., Yildirim, F., Meisel, A., Marschenz, S., 2015. Inhibition of histone methyltransferases SUV39H1 and G9a leads to neuroprotection in an in vitro model of cerebral ischemia. J Cereb Blood Flow Metab 35, 1640-1647.

Shankar, S.R., Bahirvani, A.G., Rao, V.K., Bharathy, N., Ow, J.R., Taneja, R., 2013. G9a, a multipotent regulator of gene expression. Epigenetics 8, 16-22.

Shinkai, Y., Tachibana, M., 2011. H3K9 methyltransferase G9a and the related molecule GLP. Genes Dev. 25, 781-788.

Slack, J.M., 2007. Metaplasia and transdifferentiation: from pure biology to the clinic. Nat. Rev. Mol. Cell Biol. 8, 369-378.

Subbanna, S., Basavarajappa, B.S., 2014. Pre-administration of G9a/GLP inhibitor during synaptogenesis prevents postnatal ethanol-induced LTP deficits and neurobehavioral abnormalities in adult mice. Exp Neurol 261, 34-43.

Subbanna, S., Nagre, N.N., Shivakumar, M., Umapathy, N.S., Psychoyos, D., Basavarajappa, B.S., 2014. Ethanol induced acetylation of histone at G9a exon1 and G9a-mediated histone H3 dimethylation leads to neurodegeneration in neonatal mice. Neuroscience 258, 422-432.

Subbanna, S., Shivakumar, M., Umapathy, N.S., Saito, M., Mohan, P.S., Kumar, A., Nixon, R.A., Verin, A.D., Psychoyos, D., Basavarajappa, B.S., 2013. G9a-mediated histone methylation regulates ethanol-induced neurodegeneration in the neonatal mouse brain. Neurobiol Dis 54, 475-485.

Thiel, G., Ekici, M., Rossler, O.G., 2015. RE-1 silencing transcription factor

(REST): a regulator of neuronal development and neuronal/endocrine function. Cell Tissue Res. 359, 99-109.

Wang, X., Hu, X., Yang, Y., Takata, T., Sakurai, T., 2016. Nicotinamide mononucleotide protects against beta-amyloid oligomer-induced cognitive impairment and neuronal death. Brain Res 1643, 1-9.

Wang, Z., Yang, D., Zhang, X., Li, T., Li, J., Tang, Y., Le, W., 2011. Hypoxia-induced down-regulation of neprilysin by histone modification in mouse primary cortical and hippocampal neurons. PLoS One 6, e19229.

Woodbury, D., Schwarz, E.J., Prockop, D.J., Black, I.B., 2000. Adult rat and human bone marrow stromal cells differentiate into neurons. J. Neurosci. Res. 61, 364-370.

Zhao, Q.H., Wang, S.G., Liu, S.X., Li, J.P., Zhang, Y.X., Sun, Z.Y., Fan, Q.M., Tian, J.W., 2013. PPARgamma forms a bridge between DNA methylation and histone acetylation at the C/EBPalpha gene promoter to regulate the balance between osteogenesis and adipogenesis of bone marrow stromal cells. FEBS J. 280, 5801-5814.

Zheng, D., Zhao, K., Mehler, M.F., 2009. Profiling RE1/REST-mediated histone modifications in the human genome. Genome Biol. 10, R9.

Zhou, Q., Obana, E.A., Radomski, K.L., Sukumar, G., Wynder, C., Dalgard, C.L., Doughty, M.L., 2016. Inhibition of the histone demethylase Kdm5b promotes neurogenesis and derepresses Reln (reelin) in neural stem cells from the adult subventricular zone of mice. Mol Biol Cell 27, 627-639.

감사의 글

학부생의 신분으로 실험실에 들어와 학석 연계과정을 시작하고 석사학위로 입학하여 실험실 생활을 한지 어느덧 3년이라는 시간이 흐르고 졸업을 앞둔 지금 제 주변에서 응원과 많은 조언을 해주신 교수님들과 선후배 여러분들께 감사의 말을 전하고자 글을 씁니다. 가장 먼저 부족한 저를 좋은 연구를 할 수 있게 이끌어주신 저의 지도교수님이신 조광원 교수님께 감사하다는 말 전해드립니다. 제가 실험실에 흥미를 갖을 수 있게 항상 좋은 강의 해주신 이준식 교수님 열정적이고 파워풀한 강의를 해주시고 연구를 하는데 필요한 열린 생각을 갖게 해주신 전택중 교수님 항상 따듯한 말과 격려를 아끼지 않으셨던 송상기 교수님 학생들의 건장을 우선으로 생각하시던 박현용 교수님 제 평생지도 교수님으로서 학부 1학년때부터 좋은 진로 상담을 해 주셨던 이현화 교수님 학생들과 항상 친밀하고 좋은 교류를 하려고 노력하시는 정민주 교수님 항상 밝은 표정으로 저에게 인사를 해주신 조태오 교수님 학생들을 가장 먼저 생각해 주시는 이정섭 교수님 언제나 저에게 열심히 한다라고 밝은 웃음을 지어 주시던 정현숙 교수님 인자하신 윤성명 교수님 저희 실험실에 많은 도움을 주신 온탁범 교수님 좋은 조언과 좋은 강의를 해주신 박윤경 교수님 그 외에 다른 모든 교수님들께도 감사하다는 말 전해드립니다. 중학교부터 대학원까지 한결 같은 저의 선배 신구형 제가 실험실에서 잘 생활할 수 있게 격려해주고 도와주셔서 감사합니다. 유머러스한 말로 항상 재밌게 해주었던 윤서형 감사합니다. 나의 대학교 첫 후배이자 대학원 선배인 이슬아 나한테 실험 가르쳐 주고 여러 가지 팁도 주고 많이 도와줘서 고마워 내가 대학 선배라 가르치는데 불편함도 많았을텐데 많이 양보해주고 이해해줘서 고마워 내 대학원 동기 민지야 나를 가장 많이 위로해주고 격려해준 건 너 인거 같아 내가 힘들어 할 때 마다 먼저 물어봐 주고 힘 낼 수 있게 도와준거 너무 고맙고 같이 맛있는거 먹으로 다니면서 스트레스 풀었던게 정말 그리울 것 같고 기억에 남을 거 같아 넌 마음씨가 좋으니까 어딜 가서도 잘 지낼거고 좋은 사람들도 많이 만날 수 있을거야 파이팅! 우리 실험실의 분위기 메이커였던 다희야 너가 있어서 실험실 분위기가 항상 밝았던게 아닐까

하는 생각이 들어 너도 많이 힘들고 지칠때도 있었을 텐데 항상 밝은 모습으로 긍정적인 마인드로 좋은 에너지 줘서 고맙고 실험 배울때도 열정적이고 활기차게 잘 배워줘서 고마워 앞으로 어디서든 그런 모습 잃지 말고 잘 생활하길 바랄게, 실험에 대한 관심도 많고 지식도 많은 영찬아 앞으로 걱정이 많을 것 같은데 다 잘 될거야 힘내! 우리 실험실 막내 향이야 항상 재밌는 장기를 보여줘서 고마워 졸업 준비로 바쁘고 지칠 때 너의 재밌는 장기자랑 덕분에 많이 웃었던 것 같아 고맙다. 그 외에도 저에게 좋은 정보와 지식을 주신 김미은 박사님 사회생활에 대한 팁과 충고를 많이 해준 미래누나 나의 대학원 동기들 신동엽, 김혜선, 박푸름 후배들 윤영빈, 이방헌, 정인애, 박병규, 김요한, 장현웅, 양준형 조순효, 조준휘, 한우창 대학 동기들 나주용, 채병철, 제갈현, 권기봉, 김효준, 임수민, 오정훈, 최동호, 박철웅, 염민아, 쵸효문, 최영윤, 김은정, 오다혜, 김라리 다들 고맙고 나를 지금까지 건강하고 바르게 키워주신 엄마 아빠 나 때문에 속상하고 힘든일 많았을 텐데 항상 나를 먼저 걱정해주고 아껴줘서 너무너무 고맙고 말로는 표현하지 못할 만큼 사랑합니다. 그리고 내가 가장 편하게 상담도 하고 투정도 부릴 수 있는 우리 누나! 나를 동생으로서 많이 아껴주고 챙겨줘서 너무 고마워 항상 손자 생각뿐이신 우리 할머니 그 외에 고모들과 이모들 삼촌들 친척들 모두 감사합니다.
마지막으로 나의 평생지기들 김진욱, 김지환, 김태균, 염현우, 이민혁, 박세환, 손용규 너희들이 없었다면 내가 지금까지 버틸 수 있었을까? 하는 생각이 든다. 너희한테는 말로 다 표현하지 못할 만큼 고마워~ 앞으로도 우리 우정 변치말자 친구들아 사랑한다!
지금까지 저를 아껴주고 사랑해주신 모든 사람들에게 감사합니다.